

# Protoneutron Stars with Kaon Condensation and their Delayed Collapse

Masatomi Yasuhira and Toshitaka Tatsumi

*Department of Physics, Kyoto University,*

*Kitashirakawa-Oiwake-cho,*

*Kyoto 606-8502, Kyoto, JAPAN*

*e-mail: yasuhira@ruby.scphys.kyoto-u.ac.jp*

## Abstract

Properties of protoneutron stars are discussed in the context of kaon condensation. Thermal and neutrino-trapping effects are very important ingredients to study them. By solving the TOV equation, we discuss the static properties of protoneutron stars and the possibility of the delayed collapse during their evolution.

PACS: 11.30.Rd, 12.39.Fe, 13.75.Jz, 21.65.+f, 26.60.+c, 97.60.Jd

Keywords: neutron stars, delayed collapse, kaon condensation, chiral symmetry, protoneutron stars, low-mass black holes

## I. INTRODUCTION

A protoneutron star (PNS), which is formed after the gravitational collapse of massive stars, consists of hot and dense hadronic matter. At birth the matter is lepton rich due to the trapping of neutrinos and has entropy per baryon of order 1-3 in units of Boltzmann constant. A PNS evolves in a few tens of seconds through the deleptonization and initial cooling eras to usual cold neutron stars [1]. During the evolution, some of the stars may become to be gravitationally unstable due to some hadronic phase transitions and collapse to the low-mass black holes [2], which we call the delayed collapse.

To make the low-mass black hole with the gravitational mass of  $O(1.4M_{\odot})$ , first, the maximum mass of a PNS must be sufficiently low, and secondly, the mass must exceed the maximum-mass during their evolution due to neutrino emission, cooling and/or fall-back of matter. The possibility of making the low-mass black holes in supernovae and its relation with SN1987A has been discussed by many authors [3]. The observation of neutrinos from SN1987A suggested a formation of a PNS in it. However the neutron star has never been detected so far. One idea to resolve this mystery is that the neutron star must have collapsed further into a low-mass black hole at some later time because of either the accretion of a sufficient fall-back mass and/or some change of its equation of state(EOS)

Thus it is very important to study the change of EOS during the evolution of a PNS to discuss the possibility of the delayed collapse: the EOS depends on what kind of hadronic phase transitions takes place: quark matter, boson condensed matter, hyperonic matter and so on [1]. There neutrino-trapping and thermal effects play important roles in the rearrangement of constituents of matter and they are also crucial for whether phase transition occurs or not. Numerical simulations to describe the evolution of a PNS and the delayed collapse have been done [4] [5] [6] [7]. In this paper we study kaon condensation in hot and neutrino-trapping matter, which may be a key object to the delayed collapse due to the large softening of the EOS [2] [8].

Kaon condensation has been studied by many authors mainly at zero temperature [10],

since first suggested by Kaplan and Nelson [9]. Its implications have been also discussed mainly in the context of cold neutron stars; maximum-mass, cooling mechanism, rapidly rotating pulsars and so on. Baumgarte et al. [4] performed a numerical simulation of the evolution of a PNS by taking into account the change of EOS due to kaon condensation and examined how they collapse to black holes. However they used the EOS for kaon condensed matter at *zero* temperature. There has been no study to treat the thermal effect consistently in the chiral model.

Recently we have presented a new framework to treat thermal and quantum fluctuations around the condensate on the basis of chiral symmetry [11] [12] [13]. Making full use of the group structure of chiral manifold, we have derived the thermodynamic potential from the nonlinear chiral Lagrangian. The Goldstone mode arises from the V-spin symmetry breaking there. We have found the dispersion relation for this mode, and that it plays an important role at finite temperature [14]. Here we study the kaon condensation at finite temperature using the chiral model and discuss the properties of the PNS.

There are many studies about the kaon condensation at finite temperature by using the meson-exchange model [1] [15]. Earlier work suggested that the thermal effect on the EOS is relatively small compared with the neutrino-trapping effect [1]. Pons et al. also discussed the EOS for kaon condensed matter and properties of the PNS [15]. They concluded the thermal effect is a key object to induce the delayed collapse. The most important difference between the meson-exchange model and the chiral model we use here is about the nonlinearity of the kaon field. Since the chiral symmetry dictates the nonlinear Lagrangian for the kaon field, the properties of the well-developed kaon condensed phase become very different between both models, while those are almost the same as far as the condensate is weak [1] [15]. As we shall see in this paper the chiral model gives a rather stronger condensation in comparison with the meson-exchange model. Thereby the chiral model may give a qualitatively different scenario for the delayed collapse of the PNS.

It is found that a normal PNS without any phase transition cannot collapse under no accretion and the delayed collapse is possible by the neutrino-trapping effect in the delep-

tonization era due to the occurrence of kaon condensation using a most reasonable parameter for the  $KN$  sigma term. We find that the neutrino-trapping effect gives a main contribution to the delayed collapse rather than the thermal effect, within the chiral model. We also find, with different parameters, that the thermal effect may be important as well as the neutrino-trapping effect.

In Sect.II we briefly review the essential part of the formulation that enables us to treat thermal and quantum fluctuations around the condensate transparently.

In Sect.III we discuss some features of EOS in the chiral model and the properties of a PNS, especially the possibility of its delayed collapse.

Summary and concluding remarks are given in Sect.IV.

## II. FORMULATION

Recently we have presented a framework to take into account the quantum and/or thermal fluctuations around the condensate, in accordance with chiral symmetry [11] [12] [13]. The effective partition function  $Z_{chiral}$  at temperature  $T$  can be written as

$$Z_{chiral} = N \int [dU][dB][d\bar{B}] \exp \left[ \int_0^\beta d\tau \int d^3x \{ \mathcal{L}_{chiral}(U, B) + \delta\mathcal{L}(U, B) \} \right], \quad (1)$$

with the imaginary time  $\tau = it$  and  $\beta = 1/T$ .  $\mathcal{L}_{chiral}(U, B) = \mathcal{L}_0(U, B) + \mathcal{L}_{SB}(U, B)$  is the Kaplan Nelson Lagrangian [9] and is represented with the octet baryon field,  $B$ , and the chiral field,  $U = \exp[2iT_a\phi_a/f] \in SU(3)$ , with  $SU(3)$  generators  $T_a$  and the Goldstone fields  $\phi_a$ .  $\delta\mathcal{L}$  is the induced SB term as a result of introduction of chemical potentials,  $\mu_K$  and  $\mu_n$ ,

$$\begin{aligned} \delta\mathcal{L} = & -\frac{f^2\mu_K}{4} \text{tr} \left\{ [T_{em}, U] \frac{\partial U^\dagger}{\partial \tau} + \frac{\partial U}{\partial \tau} [T_{em}, U^\dagger] \right\} \\ & - \frac{\mu_K}{2} \text{tr} \left\{ B^\dagger [(\xi^\dagger [T_{em}, \xi] + \xi [T_{em}, \xi^\dagger]), B] \right\} \\ & - \frac{f^2\mu_K^2}{4} \text{tr} \{ [T_{em}, U] [T_{em}, U^\dagger] \} + \mu_n \text{tr} \{ B^\dagger B \} - \mu_K \text{tr} \{ B^\dagger [T_{em}, B] \} \end{aligned} \quad (2)$$

with  $U = \xi^2$  and  $T_{em} = \text{diag}(2/3, -1/3, -1/3)$ . Generally it is complicated to perform the path integral by separating the fields  $\phi_a$  into the sum of classical fields  $\langle \phi_a \rangle$  and fluctuation fields  $\tilde{\phi}_a$  in the standard way, because  $\{\phi_a\}$  reside on the curved manifold

$SU(3) \times SU(3)/SU(3)$ . Instead, we introduce the local coordinates around the condensed point to eliminate the curvature effect in the neighborhood, which is equivalent to the following parameterization for  $U$ ;

$$U = \zeta U_f \zeta (\xi = \zeta U_f^{1/2} u^\dagger = u U_f^{1/2} \zeta), \quad \zeta = \exp(\sqrt{2}i\langle M \rangle / f), \quad (3)$$

where  $\langle M \rangle$  represents the condensate,  $\langle M \rangle = V_+ \langle K^+ \rangle + V_- \langle K^- \rangle$ , with  $K^\pm = (\phi_4 \pm i\phi_5)/\sqrt{2}$  and  $\theta^2 \equiv 2K^+K^-/f^2$ , while  $U_f = \exp[2iT_a\phi_a/f]$  means the fluctuation field. It may be interesting to see that this procedure can be also regarded as the separation of the zero-mode [16].

Accordingly, defining a new baryon field  $B'$  by way of

$$B' = u^\dagger B u, \quad (4)$$

we can see eventually that

$$\begin{aligned} \mathcal{L}_{chiral}(U, B) &= \mathcal{L}_0(U_f, B') + \mathcal{L}_{SB}(\zeta U_f \zeta, u B' u^\dagger), \\ \delta\mathcal{L}(U, B) &= \delta\mathcal{L}(\zeta U_f \zeta, u B' u^\dagger). \end{aligned} \quad (5)$$

Thus only the SB terms *prescribe* the  $KN$  dynamics in the condensed phase; we can easily see that the  $KN$  sigma terms,  $\Sigma_{K_i}(i = n, p)$ , stem from  $\mathcal{L}_{SB}$ , while the Tomozawa-Weinberg term from  $\delta\mathcal{L}$  [11] [13]. The sigma terms can be written by the parameters in the nonlinear chiral Lagrangian( $a_1, a_2, a_3$ ) and strange quark mass( $m_s$ ):

$$\begin{aligned} \Sigma_{Kp} &= -(a_1 + a_2 + 2a_3)m_s, \\ \Sigma_{Kn} &= -(a_2 + 2a_3)m_s. \end{aligned} \quad (6)$$

Mass differences of hadrons can determine  $a_1 m_s = -67$  MeV and  $a_2 m_s = 134$  MeV. There remains a large uncertainty associated with the coefficient  $a_3 m_s$ . Empirically  $a_3 m_s$  lies in the range  $-134$  to  $-310$  MeV, while lattice gauge simulations provide  $a_3 m_s = -(220 \pm 40)$  MeV [17] [18]. Later we mainly use  $a_3 m_s = -222$  MeV as a most reasonable value and add some results for the weak limit  $a_3 m_s = -134$  MeV to see the parameter dependence.

The integration measure is properly approximated as  $[dU_f] \simeq \prod_{a=1}^8 [d\phi_a]$  in the neighborhood of the condensate and finally we find

$$Z_{chiral} \simeq \int \prod_{a=1}^8 [d\phi_a][dB'][d\bar{B}'] \exp \left[ \int_0^\beta d\tau \int d^3x \mathcal{L}_{chiral}^{eff}(\zeta, U_f, B') \right], \quad (7)$$

with the effective chiral Lagrangian,  $\mathcal{L}_{chiral}^{eff}(\zeta, U_f, B') = \mathcal{L}_0(U_f, B') + \mathcal{L}_{SB}(\zeta U_f \zeta, u B' u^\dagger) + \delta\mathcal{L}(\zeta U_f \zeta, u B' u^\dagger)$ .

We then evaluate the partition function  $Z_{chiral}$  up to the one-loop level under the Hartree approximation for kaon-nucleon interactions; we need not care about the nucleon loops in the heavy baryon limit (HBL), which we hereafter use in this paper.

During this course, the poles of the thermal Green function for kaons give the excitation spectra of kaonic modes with energies ( $E_\pm$ ). The mode with  $E_-$  is the Goldstone mode and exhibits the Bogoliubov spectrum, which stems from the spontaneous breaking of  $V$ -spin symmetry in the condensed phase. It gives a large contribution to the thermodynamic quantities through the Bose-Einstein distribution function. Under the relevant approximation, they are reduced to the simple form

$$E_\pm(\mathbf{p}) \simeq \sqrt{p^2 + \cos\langle\theta\rangle m_K^{*2} + b^2} \pm (b + \cos\langle\theta\rangle \mu_K), \quad (8)$$

where  $m_K^{*2} = m_K^2 - \rho_B/f^2(\Sigma_{Kp}x + \Sigma_{Kn}(1-x))$  and  $b = \rho_B(1+x)/(4f^2)$ . We use this form in the following calculations. We have discussed its relevance in the previous papers [13] and have seen its practical usefulness in giving the thermodynamic quantities.

Eventually the effective thermodynamic potential  $\Omega_{chiral} = -T \ln Z_{chiral}$  reads

$$\Omega_{chiral} = \Omega_c + \Omega_K^{th} + \Omega_N, \quad (9)$$

where  $\Omega_c$  is the classical kaon contribution,

$$\Omega_c = V[-f^2 m_K^2 (\cos\langle\theta\rangle - 1) - 1/2 \cdot \mu_K^2 f^2 \sin^2\langle\theta\rangle], \quad (10)$$

and the thermal kaon contribution, is given as follows;

$$\Omega_K^{th} = TV \int \frac{d^3p}{(2\pi)^3} \ln(1 - e^{-\beta E_+(\mathbf{p})})(1 - e^{-\beta E_-(\mathbf{p})}). \quad (11)$$

It is to be noted that the zero-point-energy contribution of kaons is very small [19] [20] and we discard it in this paper.

$\Omega_N$  denotes the nucleon contribution. In order to reproduce the bulk property of nuclear matter and get a realistic EOS for kaon condensed matter, we should take into account nucleon-nucleon interactions. Following Prakash et al. [21] we introduce the potential energy in the form,

$$E_N^{pot} = E_N^{sym} + E_N^V, \quad (12)$$

where  $E_N^{sym}$  represents the symmetry energy contribution and  $E_N^V$  the residual potential contribution. The symmetry energy is given by

$$E_N^{sym} = V\rho_B(1 - 2x)^2 S^{pot}(u); \quad (u = \rho_B/\rho_0; \rho_0 = 0.16\text{fm}^{-3}) \quad (13)$$

where the function  $S^{pot}(u)$  reads,

$$S^{pot}(u) = (S_0 - (2^{2/3} - 1)(3/5)E_F^0)F(u) \quad (14)$$

with the constraint  $F(u = 1) = 1$  to reproduce the empirical symmetry energy  $S_0 \simeq 30\text{MeV}$  at the nuclear density  $\rho_0$ .  $E_F^0$  is the fermi energy at  $\rho_0$ . Hereafter we use  $F(u) = u$  for an example. It is well-known that the nuclear symmetry energy, which stems from the kinetic and potential energies, plays an important role for the ground-state properties of the condensed phase. Since we have already included the kinetic energy for nucleons, we must take into account only the potential energy contribution, which should be beyond chiral dynamics.

On the other hand, as another potential contribution besides the symmetry energy we use the following formula which simulates the results given by sophisticated theoretical calculations [21],

$$E_N^V/V = \frac{1}{2}Au^2\rho_B + \frac{Bu^{\sigma+1}\rho_B}{1 + B'u^{\sigma-1}} + 3u\rho_B \sum_{i=1,2} C_i \left( \frac{\Lambda_i}{p_F^0} \right)^3 \left( \frac{p_F}{\Lambda_i} - \arctan \frac{p_F}{\Lambda_i} \right). \quad (15)$$

We choose the parameter set  $(A, B, B', \sigma, C_i, \Lambda_i)$  for compression modulus to be  $K_0 = 240\text{MeV}$

for normal nuclear matter <sup>1</sup>. Strictly speaking, the effective potential functions Eqs.(13),(15) should include temperature dependence by way of the Pauli blocking effect on nucleon-nucleon scattering in matter. However, as has been shown in ref. [22] temperature-dependence should be weak up to several tens of MeV, so that we can use the form  $E_N^{pot}$  even at finite temperature.

Including the potential contribution  $E_N^{pot}$ , we get the single particle energies,

$$\begin{aligned}\epsilon_p(\mathbf{p}) &= \frac{p^2}{2M} - (\Sigma_{Kp} + \mu_K)(1 - \cos\langle\theta\rangle) + \frac{1}{V} \frac{\partial E_N^{pot}}{\partial \rho_p}, \\ \epsilon_n(\mathbf{p}) &= \frac{p^2}{2M} - (\Sigma_{Kn} + \mu_K/2)(1 - \cos\langle\theta\rangle) + \frac{1}{V} \frac{\partial E_N^{pot}}{\partial \rho_n}.\end{aligned}\quad (16)$$

We have used the non-relativistic approximation for nucleons, where the scalar density is not distinguished from the ordinary density  $\rho_i$ .

Then nucleon contributions can be written in the form;

$$\Omega_N = \Omega_N^{kin} + \Omega_N^{pot}, \quad (17)$$

where  $\Omega_N^{kin}$  is the ‘‘kinetic energy’’ contribution and  $\Omega_N^{pot}$  the ‘‘potential energy’’ contribution,

$$\begin{aligned}\Omega_N^{kin} &\simeq -2TV \sum_{n,p} \int \frac{d^3p}{(2\pi)^3} \ln(1 + e^{-\beta(\epsilon_i(\mathbf{p}) - \mu_i)}), \\ \Omega_N^{pot} &= -\rho_B \frac{\partial E_N^{pot}}{\partial \rho_B}.\end{aligned}\quad (18)$$

Here it is useful to introduce the new parameters  $\mu_i^0$  ( $i = n, p$ ) instead of the chemical potentials  $\mu_i$ ,

$$\begin{aligned}\mu_p^0 &= \mu_p + (\mu_K + \Sigma_{Kp})(1 - \cos\langle\theta\rangle) - \frac{1}{V} \frac{\partial E_N^{pot}}{\partial \rho_p}, \\ \mu_n^0 &= \mu_n + \left(\frac{\mu_K}{2} + \Sigma_{Kn}\right)(1 - \cos\langle\theta\rangle) - \frac{1}{V} \frac{\partial E_N^{pot}}{\partial \rho_n}.\end{aligned}\quad (19)$$

Then  $\Omega_N^{kin}$  can be written in the simple form,

---

<sup>1</sup> Since this parameter set has been also used in Ref. [17] in which  $V(u)$  corresponds to our expression  $E_N^V$ , our results at zero temperature are the same as theirs.



$$\Omega_N^{kin} \simeq -2TV \sum_{n,p} \int \frac{d^3p}{(2\pi)^3} \ln(1 + e^{-\beta(\epsilon^0(\mathbf{p}) - \mu_i^0)}), \quad (20)$$

with the “free” kinetic energy  $\epsilon^0(\mathbf{p}) = p^2/2M$ .

Using the thermodynamic relations,

$$S_{chiral} = -\frac{\partial \Omega_{chiral}}{\partial T}, \quad Q_i = -\frac{\partial \Omega_{chiral}}{\partial \mu_i}, \quad E_{chiral} = \Omega_{chiral} + TS_{chiral} + \sum \mu_i Q_i, \quad (21)$$

we can find charge, entropy and internal energy. The entropy is given by

$$\begin{aligned} S_{chiral} = & -\beta \Omega_{chiral} + \beta V f^2 \left( -\frac{1}{2} \mu_K^2 \sin^2 \langle \theta \rangle + m_K^2 (1 - \cos \langle \theta \rangle) \right) \\ & + \beta V \int \frac{d^3p}{(2\pi)^3} [E_-(\mathbf{p}) f_B(E_-(\mathbf{p})) + E_+(\mathbf{p}) f_B(E_+(\mathbf{p}))] \\ & + 2\beta V \sum_{n,p} \int \frac{d^3p}{(2\pi)^3} [(\epsilon^0(\mathbf{p}) - \mu_i^0) f_F(\epsilon^0(\mathbf{p}) - \mu_i^0)] \\ & - \beta V (1 - 2x)^2 S^{pot}(u) \rho_B, \end{aligned} \quad (22)$$

with the Fermi-Dirac distribution function  $f_F(E)$  and the Bose-Einstein distribution function  $f_B(E)$ . The kaonic charge is given by,

$$Q_K = V \left[ \mu_K f^2 \sin^2 \langle \theta \rangle + \cos \langle \theta \rangle n_K + (1 + x) \sin^2(\langle \theta \rangle / 2) \rho_B \right], \quad (23)$$

with the number density of thermal kaons  $n_K$ ,

$$n_K = \int \frac{d^3p}{(2\pi)^3} [f_B(E_-(\mathbf{p})) - f_B(E_+(\mathbf{p}))]. \quad (24)$$

Nucleon charges are given by

$$Q_i = 2V \int \frac{d^3p}{(2\pi)^3} [f_F(\epsilon^0(\mathbf{p}) - \mu_i^0)], \quad (i = n, p). \quad (25)$$

Then the total energy is given by

$$\begin{aligned} E_{chiral} = & V f^2 \left( -\frac{1}{2} \mu_K^2 \sin^2 \langle \theta \rangle + m_K^2 (1 - \cos \langle \theta \rangle) \right) \\ & + V \int \frac{d^3p}{(2\pi)^3} [E_-(\mathbf{p}) f_B(E_-(\mathbf{p})) + E_+(\mathbf{p}) f_B(E_+(\mathbf{p}))] \\ & + 2V \sum_{n,p} \int \frac{d^3p}{(2\pi)^3} \left[ \left( \epsilon_i(\mathbf{p}) - \frac{1}{V} \frac{\partial E_N^{pot}}{\partial \rho_n} \right) f_F(\epsilon^0(\mathbf{p}) - \mu_i^0) \right] \\ & + V (1 - 2x)^2 S^{pot}(u) \rho_B + \mu_K Q_K, \end{aligned} \quad (26)$$

where we add the term with  $\frac{1}{V} \frac{\partial E_N^{pot}}{\partial \rho_n}$ , to avoid double-counting.

The total thermodynamic potential  $\Omega_{total}$  is given by adding the one for leptons (electrons, muons and neutrinos),  $\Omega_l$ ,  $\Omega_{total} = \Omega_{chiral} + \Omega_l$ ;

$$\Omega_l = -2TV \sum_{e,\mu,\nu} \int \frac{d^3p}{(2\pi)^3} \left[ \ln(1 + e^{-\beta(\epsilon_i(\mathbf{p}) - \mu_i)}) + \ln(1 + e^{-\beta(\epsilon_i(\mathbf{p}) + \mu_i)}) \right], \quad (27)$$

with  $\epsilon_i(\mathbf{p}) = \epsilon_{\bar{i}}(\mathbf{p}) = \sqrt{m_i^2 + p^2}$  ( $i = e, \mu, \nu_e, \nu_\mu$ ).

The parameters  $x, \langle \theta \rangle$  and chemical potentials  $\mu_K, \mu_i (i = n, p)$  are determined by the extremum conditions for given density and temperature. The first condition demands  $\partial \Omega_{total} / \partial x = 0$ , which is equivalent with the condition for chemical equilibrium among kaons, nucleons:

$$\mu_n - \mu_p = \mu_K, \quad (28)$$

or

$$\mu_p^0 - \mu_n^0 - 4S^{pot}(u)(1 - 2x) + \frac{1 - \cos \langle \theta \rangle}{2} \{2(\Sigma_{Kn} - \Sigma_{Kp}) - \mu_K\} + \mu_K = 0, \quad (29)$$

by way of Eq.(19). The charge neutrality demands  $\partial \Omega_{total} / \partial \mu_K = 0$ :

$$Q_K + Q_e + Q_\mu = Q_p (= xV\rho_B), \quad (30)$$

where the hadron charges are given in Eqs. (23),(25) and the lepton numbers are given by

$$Q_i \equiv Y_i \rho_B = 2V \int \frac{d^3p}{(2\pi)^3} [f_F(\epsilon_i(\mathbf{p}) - \mu_i) - f_F(\epsilon_i(\mathbf{p}) + \mu_i)], \quad (31)$$

with the lepton-number fractions  $Y_i$  ( $i = e, \mu$ ). Finally the extremum condition with respect to  $\langle \theta \rangle$  gives

$$0 = f^2 \sin \langle \theta \rangle (m_K^{*2} - 2\mu_K b - \mu_K^2 \cos \langle \theta \rangle) + \frac{\partial(\Omega_K/V)}{\partial \langle \theta \rangle}, \quad (32)$$

which is just the field equation of motion for kaon at momentum zero. Eqs.(29),(30), (32) are the basic equations to determine the equilibrated state.

We can see that once the fluctuation contribution (the second term in Eq.(32)) is taken into account, the relation  $E_-(\mathbf{p} = 0) = 0$  no longer holds. So the Goldstone nature is violated

up to one-loop order in the loop expansion. This situation always occurs in the perturbation theory [23]: the number of loops are *always* different between the thermodynamic potential ( $N_l$ ) and the self-energy for kaons ( $N_l - 1$ ). This shortcoming is never cured unless we perform a full order calculation. This matter is beyond the scope of this paper. Fortunately, the contribution of fluctuations can be estimated to be small in the temperature-density region we are interested in [13].

### III. NUMERICAL RESULTS AND DISCUSSIONS

Using the formulation given in Sect.II, we study the properties of kaon condensed matter taking into account thermal and neutrino-trapping effects and then discuss the properties of a PNS. Finally some implications on its delayed collapse will be given. In this paper, we use  $a_3 m_s = -222\text{MeV}$  ( $\Sigma_{KN} = \frac{1}{2}(\Sigma_{Kp} + \Sigma_{Kn}) = 344\text{ MeV}$ ) which is known as a most reasonable value (as discussed in Sect.II). In Sect.III D we will give some results in the case of weak coupling limit,  $a_3 m_s = -134\text{MeV}$  corresponding to  $\Sigma_{KN} = 168\text{ MeV}$  to study the dependence of the EOS on the strength of the  $KN$  interaction.

#### A. Phase Diagram

First we show the phase diagram in Fig.1 for neutrino-free and trapping matter. In the neutrino-trapping case, there exist additional conditions with respect to the conservation of lepton numbers [17]. Recent calculations of gravitational core-collapse of massive stars indicate the electron lepton number  $Y_{le}$  at the onset of neutrino-trapping  $Y_{le} \approx 0.35$  [24]. Then we take  $Y_{le} \equiv Y_e + Y_{\nu_e} = 0.4$  and  $0.3$  and for muon  $Y_{l\mu} \equiv Y_\mu + Y_{\nu_\mu} = 0.0$  in the neutrino-trapping case. On the other hand, in the neutrino-free case,  $Y_{\nu_e} = Y_{\nu_\mu} = 0$ .

## FIGURES

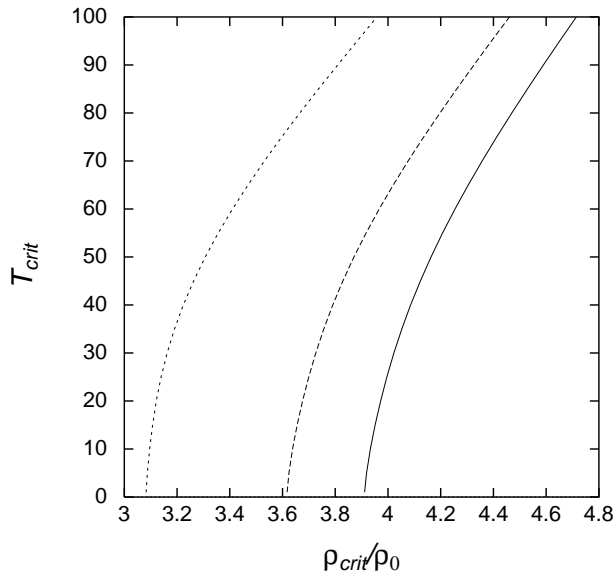


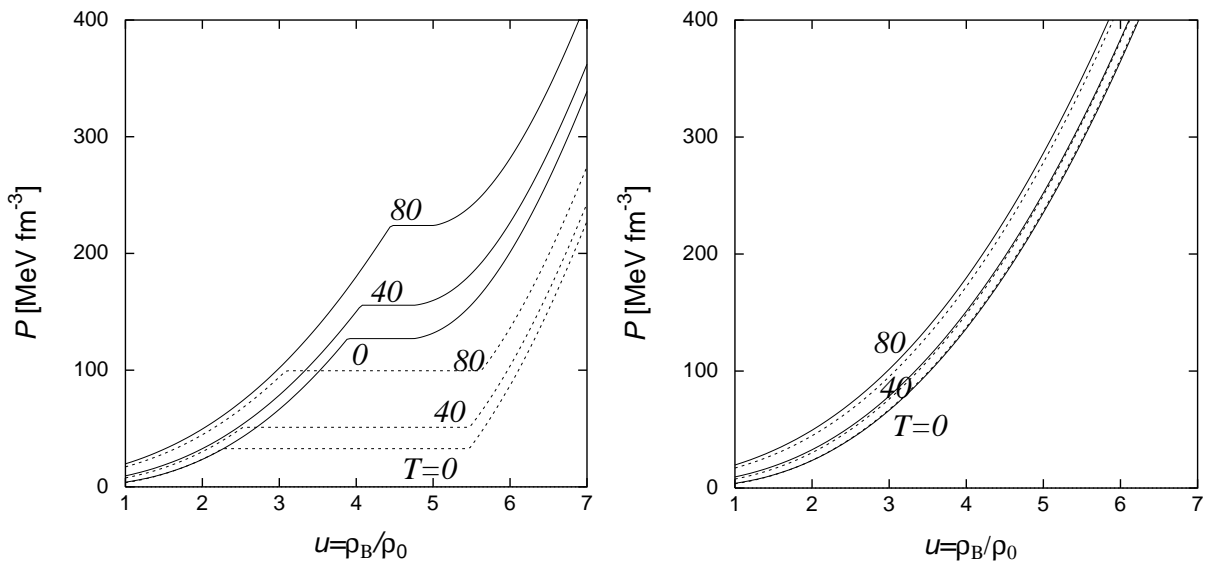
FIG. 1. Phase Diagram: solid line and dashed line show the critical lines in the neutrino-trapped cases,  $Y_{le} = 0.4$  and  $0.3$ , respectively and dotted line in the neutrino-free case.

In the phase diagram the temperature-density plane is separated into two regions by the critical line; the left-side region means normal phase, and the right-side region the kaon-condensed phase. We can see that both of the neutrino-trapping and thermal effects work against the phase transition. In the low-temperature case the neutrino-trapping effect is dominant, while both effects become comparable at high-temperature.

The neutrino-trapping effect may be simply understood as follows. Kaon condensation occurs when the lowest kaon energy ( $\epsilon_{K^-}$ ) is equal to the kaon chemical potential ( $\mu_K$ ):  $\epsilon_{K^-}$  decreases by attractive kaon-nucleon interactions as density increases, while  $\mu_K = \mu_n - \mu_p$  increases to match  $\epsilon_{K^-}$  at the critical density. In the neutrino-trapping case, the chemical equilibrium due to weak interactions implies that the relation,  $\mu_K = \mu_n - \mu_p = \mu_e - \mu_{\nu_e}$ , holds. Compared with the neutrino-free case where  $\mu_{\nu_e} = 0$ ,  $\mu_K$  should be reduced due to the finite contribution of  $\mu_{\nu_e}$ . Hence higher density is needed to satisfy the condition  $\epsilon_{K^-} = \mu_K$ .

## B. EOS for thermal and isentropic matter

Here we compare the equations of state in the two cases: the isothermal and isentropic cases. The equations of state under the isothermal condition ( $T = 0, 40$  and  $80$  MeV) for kaon condensed matter and normal matter are depicted in Fig.2. The resulting EOS for kaon condensed matter shows the existence of the thermodynamically unstable region because the phase transition is of first order and large softening of EOS so that we have recourse to the Maxwell construction to obtain the realistic EOS in equilibrium<sup>2</sup>. There appears the equal-pressure region as a result of the Maxwell construction. We can see that both the thermal and neutrino-trapping effects stiffen the EOS mainly through suppression of kaon condensate. Then, in comparison of the EOS with that for normal matter, the thermal effect is more profound, in particular around the critical density.




---

<sup>2</sup> Strictly speaking, we need to apply the Gibbs conditions because there exist two chemical potentials [25] [26]. However, we immediately see that the Gibbs conditions cannot be satisfied in the chiral model(Appendix A). So we use here the Maxwell construction for simplicity to get the EOS in equilibrium and leave this matter for a future study.

FIG. 2. Pressure of isothermal matter ( $T = 0, 40, 80\text{MeV}$ ) for kaon condensed matter [left panel] and for normal nuclear matter in beta-equilibrium [right panel]. Solid lines and dashed lines are in the neutrino-trapped case ( $Y_{le} = 0.4$ ) and the neutrino-free case, respectively.

The equal-pressure region becomes narrower as temperature increases or more neutrinos are trapped, which implies that the magnitude of the first-order phase transition is reduced by both effects of temperature and neutrinos. We can see the remarkable narrowing, especially in the neutrino-trapping case because trapped neutrinos suppress not only the occurrence of kaon condensation but also the growth of the condensate. We shall see later that the existence of the equal-pressure region may lead to the gravitationally unstable region in the branch of neutron stars.

The isentropic EOS might be more relevant for the PNS matter. First of all we show the isentropic lines in density-temperature plane in Fig.3 by calculating entropy by the use of Eq.(22) and lepton contribution for given temperature and density. In each isentropic line, nucleons dominantly contribute to entropy [1] [6] [15]. Under the isentropic condition, in which entropy per baryon ( $S$ ) is taken to be constant (1,2 or 3) over the star interior, temperature increases as density becomes high. This means that temperature becomes the highest at the center of the star once we construct a PNS with isentropic matter.

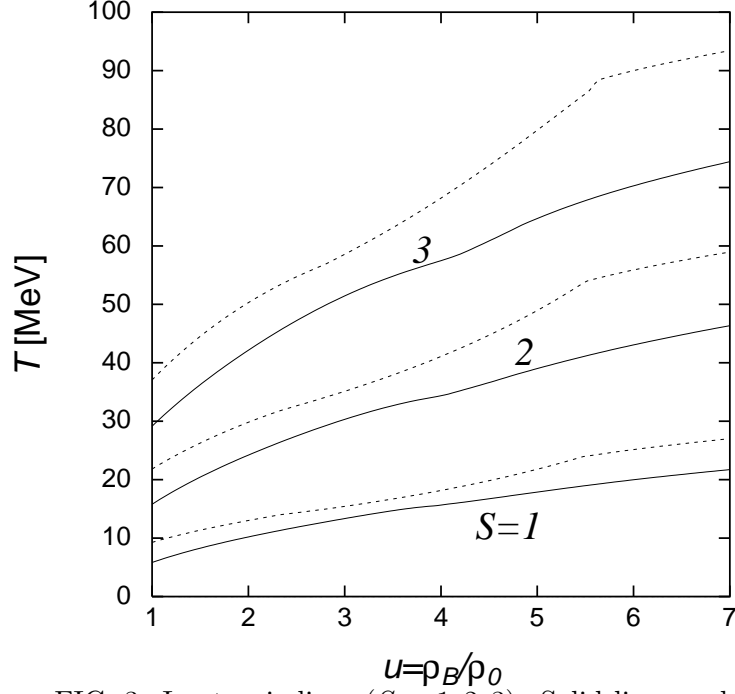


FIG. 3. Isentropic lines ( $S = 1, 2, 3$ ). Solid lines and dashed lines are in the neutrino-trapped case ( $Y_{le} = 0.4$ ), the neutrino-free case, respectively.

Then the isentropic EOS can be obtained by connecting the values of pressure at the corresponding temperatures for given densities (Fig.4). It is to be noted that the equal-pressure region, under the isentropic condition, disappears except the  $S = 0$  cases.

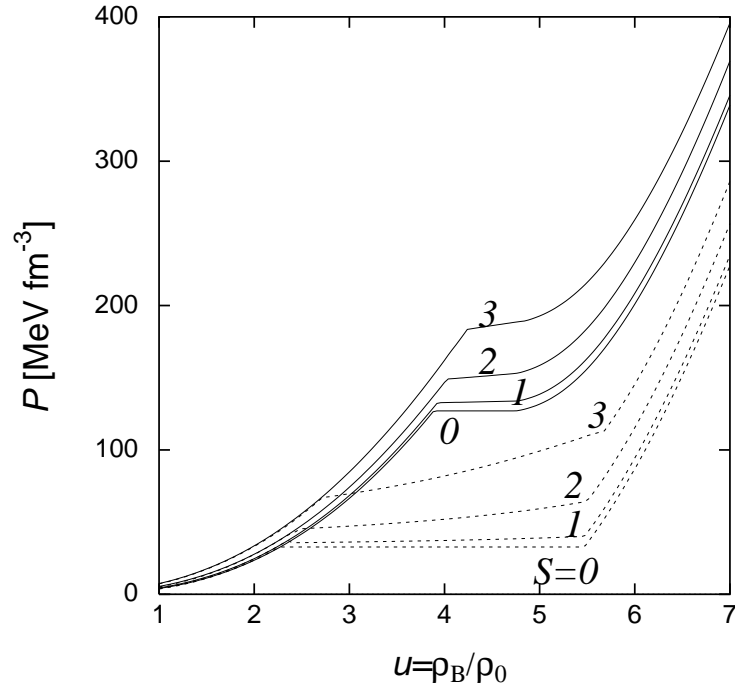


FIG. 4. Pressure for isentropic matter ( $S = 0, 1, 2, 3$ ). Solid line and dashed line are in neutrino-trapping case ( $Y_{le} = 0.4$ ) and neutrino-free case respectively.

It is well-known that when the equal-pressure region exists in the EOS, neutron star also has a density gap [27]. In the isentropic case, the equal-pressure region no longer exists and the density gap disappears even if we apply the Maxwell construction for the isothermal EOS. Instead the mixed phase appears inside the neutron star <sup>3</sup>.

### C. Properties of a PNS and the possibility of its delayed collapse

Using the isentropic EOS, we construct a PNS by solving TOV equation<sup>4</sup>. In Fig.5 we show the central density-gravitational mass relation in the neutrino-free or trapping case with entropy per baryon  $S = 0, 1, 2$  or  $3$ . We can see the thermal effect is large for the stars whose central density is around the critical density because the pressure rapidly increases in this region as temperature does. On the other hand, mass of the stars with high central density seems to be hardly changed by the thermal effect. This is because the thermal effect causes not only higher pressure but also larger energy which in turn results in the stronger gravity. Sometimes this leads to the lower maximum-mass for the higher entropy.

---

<sup>3</sup>Note that this mixed phase should be distinguished from the one resulted from the Gibbs conditions.

<sup>4</sup> In the low density region  $\rho_B < \rho_0$ , we use the EOS calculated by Lattimer et al [28].



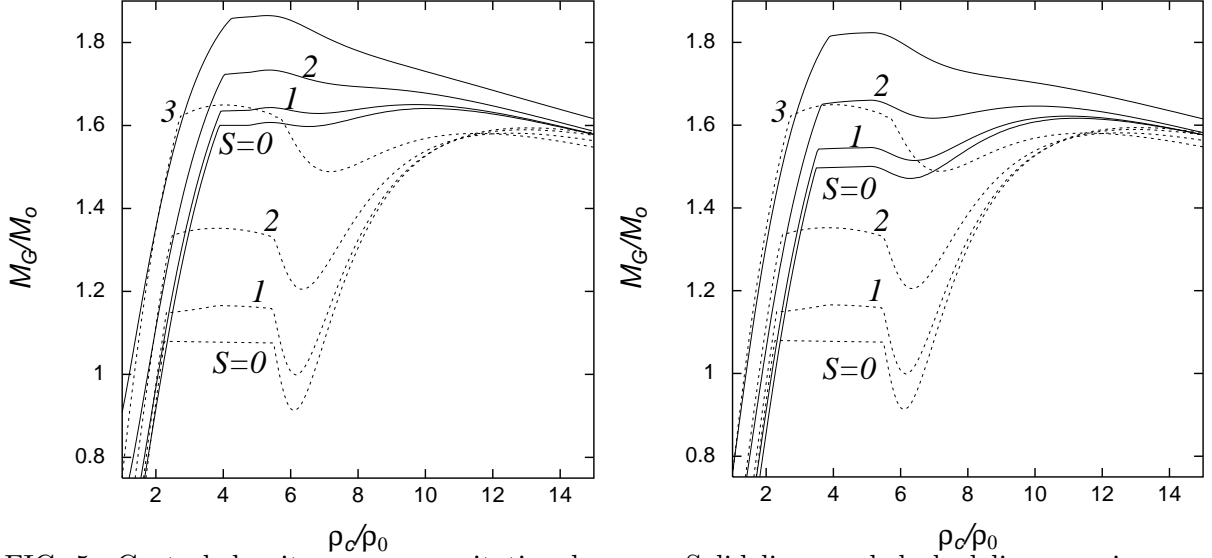


FIG. 5. Central density versus gravitational mass. Solid lines and dashed lines are in neutrino-trapping ( $Y_{le} = 0.4$ [left panel] or  $Y_{le} = 0.3$ [right panel]) and neutrino-free cases respectively at  $S = 0, 1, 2, 3$ .

We can find that, clearly in the neutrino-free case, once kaon condensation occurs in the core of a star, gravitationally unstable region (negative gradient part) appears and the neutron star branch is separated into two stable branches: one is for stars with kaon condensate in their cores and the other consisting of only normal matter. The maximum mass of the stars which include kaon condensate in the core, is hardly changed but decreases by the thermal effect because of the strong gravity except the  $S = 3$  case.

In the  $S = 0, 1$  and neutrino-trapping cases, we can see that the neutron-star branch is also separated by the gravitationally unstable region and the maximum-mass lies on the branch with kaon condensate.

On the other hand, in other cases: the  $S = 3$  and neutrino-free case, the  $S = 2, 3$  and neutrino-trapping cases, almost all of the stars with kaon condensate are gravitationally unstable, and the maximum-mass star still resides on the normal branch. For this reason the central density of the maximum-mass star is very different from those in the  $S = 0$  or  $1$  case. In table I we summarize the data for stars with maximum-mass in each case.

TABLES

	branch	central density	gravitational mass	total baryon number
<u><math>\nu</math>-free <math>Y_{\nu_e} = 0</math></u>				
$S = 0$	K	$13.2\rho_0$	$1.59M_\odot$	$2.24 \times 10^{57}$
$S = 1$	K	$13.5\rho_0$	$1.59M_\odot$	$2.22 \times 10^{57}$
$S = 2$	K	$12.5\rho_0$	$1.58M_\odot$	$2.14 \times 10^{57}$
$S = 3$	N	$4.0\rho_0$	$1.65M_\odot$	$2.11 \times 10^{57}$
<u><math>\nu</math>-trapping <math>Y_{l_e} = 0.4</math></u>				
$S = 0$	K	$10.0\rho_0$	$1.64M_\odot$	$2.13 \times 10^{57}$
$S = 1$	K	$9.6\rho_0$	$1.65M_\odot$	$2.14 \times 10^{57}$
$S = 2$	N	$5.4\rho_0$	$1.73M_\odot$	$2.23 \times 10^{57}$
$S = 3$	N	$5.3\rho_0$	$1.86M_\odot$	$2.36 \times 10^{57}$
<u><math>\nu</math>-trapping <math>Y_{l_e} = 0.3</math></u>				
$S = 0$	K	$11.3\rho_0$	$1.62M_\odot$	$2.15 \times 10^{57}$
$S = 1$	K	$11.0\rho_0$	$1.62M_\odot$	$2.14 \times 10^{57}$
$S = 2$	N	$5.1\rho_0$	$1.66M_\odot$	$2.15 \times 10^{57}$
$S = 3$	N	$5.1\rho_0$	$1.82M_\odot$	$2.33 \times 10^{57}$

TABLE I. Configuration for stars with maximum-mass: which branch the star resides in, normal branch(N) or kaon condensed branch(K), its central density, mass and total baryon number.

To discuss the possibility of the delayed collapse of the PNS, the total baryon number  $N_B$  should be fixed as a conserved quantity during the evolution [29], under the assumption that there is no accretion in the deleptonization and initial cooling eras.

Discarding gravitationally unstable stars, we show mass of stable stars for given baryon numbers in Fig.6. Each terminal point represents the star with the maximum-mass and the maximum total baryon number in each case. If the initial mass is beyond the terminal point when the neutron star is born, it should collapse into a black hole (not a delayed collapse but the usual formation of a black hole during supernova explosion). We have shown the neutrino-trapping and free cases; the former corresponds to the initial stars before the deleptonization era, while the latter to the initial cooling era after deleptonization. It is interesting to see the difference between the neutrino-free and trapping cases: the curve is shortened as entropy increases in the former case, while elongated in the latter case. The difference results from which branch the maximum-mass star resides in. These features are responsible for the following discussion about the delayed collapse and the maximum-mass of cold neutron stars.

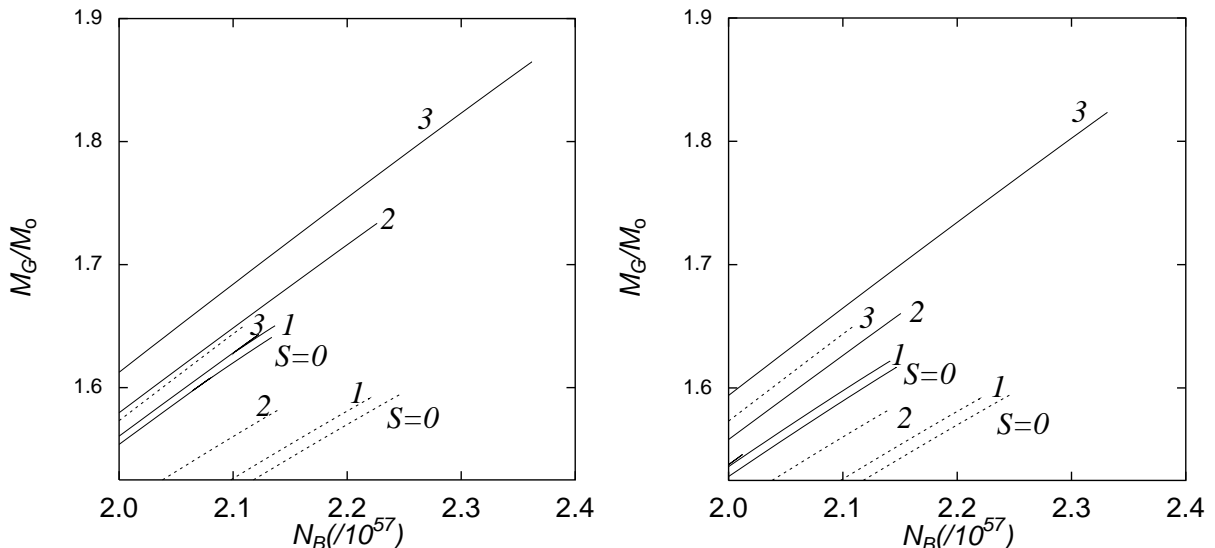


FIG. 6. Total baryon number and gravitational mass for stable PNS. Solid lines and dashed lines in neutrino-trapping ( $Y_{le} = 0.4$ [left panel] or  $Y_{le} = 0.3$ [right panel]) and neutrino-free cases, respectively at  $S = 0, 1, 2, 3$ .

The delayed collapse takes place if the initially stable star on a curve finds no correspond-

ing stable point on other curves at any stage during its evolution through deleptonization or cooling. When we discuss the evolution, several time-scales are important:  $t_K$  for the onset and growth of kaon condensation,  $t_{del}$  and  $t_{cool}$  for deleptonization and initial cooling eras, respectively. We can neglect  $t_K$  because  $t_K \ll$  several sec.  $\approx t_{del} < 20\text{-}30$  sec.  $\approx t_{cool}$  [1] [30].

Now, consider the typical evolution: for example, a PNS has initially  $Y_{le} = 0.4$  and  $S = 2$  after supernova explosion and evolves through deleptonization into the  $S = 2$  and neutrino-free stage as an intermediate stage. We can see clearly the PNS with  $1.68M_\odot \leq M_G \leq 1.73M_\odot$  can exist as meta-stable star at the beginning but cannot find any point on the curve in the  $S = 2$  and neutrino-free case. Therefore it must collapse to the low-mass black hole in the deleptonization era. It is to be noted that because the stars on the curve in the  $S = 2$  and  $Y_{le} = 0.4$  case hardly include kaon condensate, their collapse are largely due to the appearance of kaon condensate in their cores.

Furthermore, we can also determine maximum-mass of cold neutron stars by taking into account the evolution of the PNS, as pointed out by Takatsuka [29]. Usually we assign maximum-mass of cold neutron stars as the terminal point on the curve in the  $S = 0$  and neutrino-free case in Fig.6 ( $M_{max} = 1.59M_\odot$ ). However, it is wrong when we take into account the evolution of neutron stars, especially in the initial cooling era. In order to see how to determine the realistic maximum-mass of cold neutron stars, we consider a typical evolution with the total baryon number fixed. During the evolution we have already adopted, stars with more total baryon number than the terminal point of the curve in the  $S = 2$  and neutrino-free case should collapse to black-holes in the deleptonization era and cannot evolve stably to the usual cold neutron stars. Therefore only stars with the total baryon number  $N_B \leq 2.14 \times 10^{57}$  can evolve to cold neutron stars and the corresponding maximum-mass is  $1.54M_\odot$  (See Fig.6 and Table I.). Generally speaking, the maximum-mass should be determined by taking into account the evolution [29]. In our calculation it seems that the neutrino-free and hot stage plays an important role to determine the maximum-mass.

If we consider other scenarios, we can of course determine the maximum-mass of cold

neutron stars and stars which should collapse to the low mass black hole in each case.

We can conclude that the delayed collapse possibly takes place in the deleptonization era due to the occurrence of kaon condensation and the maximum-mass should be determined in the initial cooling era.

Next, we show that the delayed collapse in the case of the PNS consisting of only normal matter (without any phase transition) is impossible. In Fig.7 the gravitational mass for gravitationally stable *normal* neutron stars is plotted as a function of total baryon number. Each terminal point represents the maximum-mass star in each configuration. We can similarly study the stability of neutron stars in the deleptonization or cooling stage. After all every star can find the stable point in each stage, and the delayed collapse of *normal* neutron stars is impossible.

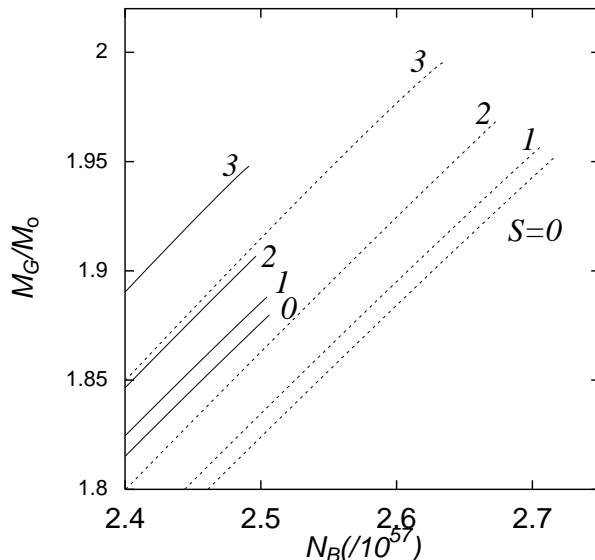


FIG. 7. Total baryon number and gravitational mass for normal matter. Solid lines and dashed lines are in neutrino-trapping ( $Y_{le} = 0.4$ ) and neutrino-free cases, respectively at  $S = 0, 1, 2, 3$ .

#### D. Case of the weak $KN$ sigma term

The left panel in Fig.8 shows the isentropic EOS for neutrino-free and trapping ( $Y_{le} = 0.4$ ) matter in the case of  $\Sigma_{KN} = 168\text{MeV}$ . The phase transition is of the second order in this case. The critical density is moved higher compared to that in the case of  $\Sigma_{KN} = 344\text{MeV}$  (See Fig.4), which leads to the weaker softening of the EOS. There is no thermodynami-

cally unstable region in the isothermal EOS and we don't need the Maxwell nor the Gibbs constructions.

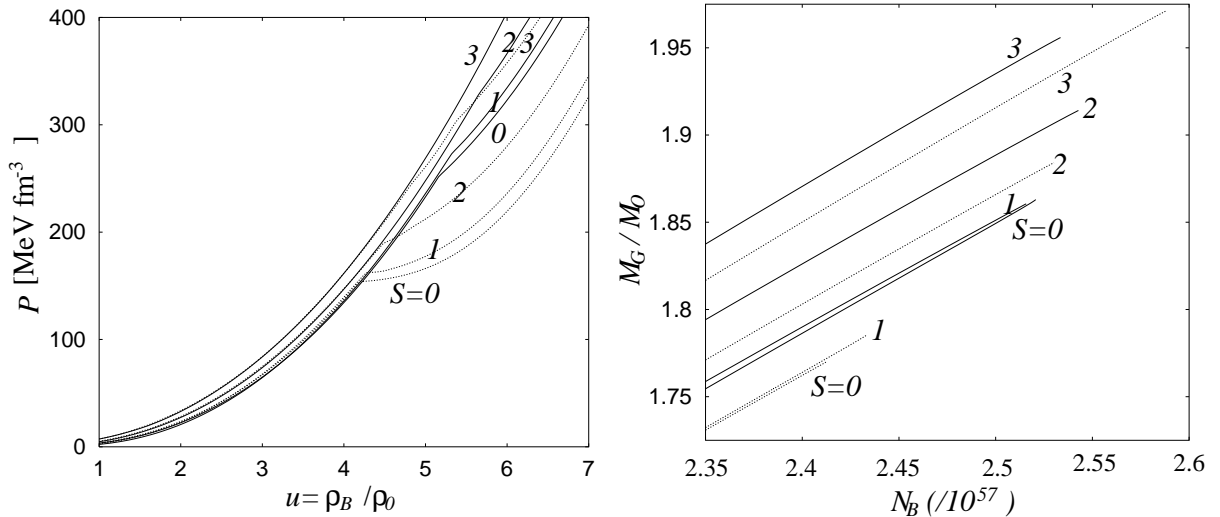


FIG. 8. The EOS [left panel] and the relation between total baryon number and gravitational mass for stable PNS [right panel] in the case of  $\Sigma_{KN} = 168\text{MeV}$ . Solid lines and dashed lines are in neutrino-trapping ( $Y_{le} = 0.3$ ) and neutrino-free case at  $S = 0, 1, 2, 3$ .

With these equations of state, properties of the PNS can be studied as well. The relations between the total baryon number and the gravitational mass are shown in the right panel in Fig.8. We can also discuss the possibility of the delayed collapse in the case of weak  $KN$  coupling. The behavior is very different from that in the case of  $\Sigma_{KN} = 344\text{MeV}$  in the left panel in Fig.6. As entropy increases, the terminal point in the neutrino-free case tends to move largely to more baryon number and heavier gravitational mass because their central densities remain around  $6\rho_0$ , where the thermal effect in the EOS are remarkable in Fig.8. On the other hand, in the neutrino-trapping case, the maximum total baryon number is hardly changed in each configuration.

Then if we assume the same evolution in the above discussion: a newly born PNS sitting on the curve in the  $S = 2$  and neutrino-trapping case evolves to the corresponding one on the curve in the  $S = 2$  and neutrino-free case, delayed collapse can occur in the deleptonization era. Moreover, it is also possible in the initial cooling era, different from the case of  $\Sigma_{KN} = 344\text{MeV}$  (See the curves in the neutrino-free case in Fig.8). Therefore

we should conclude that the thermal effect may cause the delayed collapse as well as the neutrino-trapping effect for the parameter  $\Sigma_{KN} = 168\text{MeV}$ .

#### IV. SUMMARY AND CONCLUDING REMARKS

In this paper, using our new framework based on chiral symmetry to treat the kaon condensation at finite temperature, we have discussed the properties of kaon condensed matter and its implication on astrophysics, especially the delayed collapse.

When we discard any phase transition, the delayed collapse is impossible in deleptonization and initial cooling eras. On the other hand, when kaon condensation is realized, the delayed collapse is possible. We found that, in the case of  $\Sigma_{KN} = 344\text{MeV}$ , which is a most reasonable value for the  $KN$  sigma term, the neutrino-trapping effect gives rise to the delayed collapse under no accretion of matter from the surroundings. This point is a main difference to the previous work about kaon condensation and the delayed collapse [15], in which the meson-exchange model was used and it was concluded that the thermal effect is a key object to the delayed collapse.

The difference may result from the fact that, in the chiral model, the PNS has very high central density, compared with that in the meson-exchange model [15], due to the stronger phase transition. We also studied the case of weak limit of the  $KN$  sigma term,  $\Sigma_{KN} = 168\text{MeV}$ , which is a control parameter for the strength of the phase transition in the chiral model, to confirm our findings and see to what extent they are modified by the parameter dependence. We find that the neutrino-trapping effect can cause the delayed collapse in the deleptonization era even in this case. However, we also find that the thermal effect becomes important in this limit and the delayed collapse becomes possible by the thermal effect in some scenarios. Some people may have impression that the Maxwell construction gives such high central density in the chiral model. However, we have rather high central density even in the weak coupling limit, as is seen in Sec.III D where we no longer need the Maxwell nor Gibbs construction. Hence we can say that the nonlinearity of the kaon field, which is an

essential feature of the chiral model, gives rise to a stronger phase transition than in the meson exchange model.<sup>5</sup> Thus we conclude that the delayed collapse is possible due to the occurrence of kaon condensation in the core of the PNS and neutrino-trapping effect gives a main contribution in the chiral model.

In order to study the mechanism of the delayed collapse and mass region of the PNS to collapse in more detail, we have to study the dynamical evolution beyond the static discussion given here. The accretion of a fall-back mass may be an important ingredient [3], by which the delayed collapse may occur more easily. Neutrino diffusion is another important ingredient in that study: we must treat the change of EOS, neutrino opacity and heat capacity in a consistent way which come in the diffusion equation [6] [7] [32]. Since the neutrino-nucleon scattering or neutrino absorption by nucleons should be enhanced in the kaon condensed phase [31] [33] the neutrino-trapping era might last longer if the heat capacity is little changed.

The heat capacity is related to the properties of matter at finite temperature, which should be dominated by the nucleon contribution [1] [6] [15]. In the calculations with relativistic mean field theory(RMF), the scalar interaction between kaon and nucleon and that between nucleons may give contributions through the modification of nucleon mass. The effective mass of nucleons affects the entropy or specific heat through the equation for nucleon contribution to entropy per baryon ( $S_N$ ),

$$\frac{S_N}{\pi^2 T} = \frac{x^{1/3} \sqrt{M_i^{*2} + (3\pi\rho_p)^{2/3}} + (1-x)^{1/3} \sqrt{M_i^{*2} + (3\pi\rho_n)^{2/3}}}{(3\pi^2\rho_B)^{2/3}} \quad (33)$$

with the low temperature approximation in the relativistic treatment [6] [15]. The nucleon effective mass is simply written as  $M_i^* = M - \Sigma_{Ki}(1 - \cos\langle\theta\rangle)$ , ( $i = n, p$ ) in our case, and there is no contribution from the nucleon-nucleon interaction. Then the ratio  $M_i^*/M$  remains one in the normal phase while it decreases to be 0.6-0.7 in the well-developed kaon condensed

---

<sup>5</sup>The importance of the nonlinearity is also seen in the context of the discussion about the possibility of the Gibbs construction (see Appendix A).



phase. In the realistic treatments of nuclear matter it should have density dependence even in the normal matter, so that it should be a smaller value than we have found; e.g., it has been found 0.1-0.4 within the RMF [15]. Furthermore we have treated nucleons in a non-relativistic way, so that the heat capacity is given only by their kinetic energies without any effect by the condensate. Then in the formula of entropy or specific heat the bare mass comes in instead of the effective mass and it may lead to the overestimation for specific heat. At the same time entropy may be overestimated as well; we may underestimate the thermal effect in this paper. In order to improve these points resulting from the nucleon's effective mass, we are planning to incorporate the RMF besides the chiral model for the  $KN$  interaction, as an extension from the previous work at zero temperature [27].

In this paper we studied the kaon condensation and found that the delayed collapse is possible due to not only the thermal effect but also the neutrino-trapping effect through the suppression of condensate. It is very interesting to study whether the delayed collapse occurs in the deleptonization or initial cooling era for other phase transitions, for example, hyperonic matter [6] or quark matter.

## V. ACKNOWLEDGEMENT

We thank T. Harada, K. Nakao, T. Takatsuka, T. Muto and D.N. Voskressenski for useful discussions and comments.

This work was supported in part by the Research Fellowships of the Japan Society for the Promotion of Science for Young Scientists and by the Japanese Grant-in-Aid for Scientific Research Fund of the Ministry of Education, Science, Sports and Culture(11640272).

## APPENDIX A

In this paper we have applied the Maxwell construction (MC) to get the EOS in equilibrium. Strictly speaking, we need to apply the Gibbs conditions (GC) instead of using the MC [25] because there exist two chemical potentials: baryon (neutron) and charge (electron) chemical potentials. Recently an attempt appeared along this line to derive a realistic EOS [26]. Then EOS should be smoothed due to the appearance of the *mixed phase*, where normal matter and kaon condensed matter coexist. At the beginning of the mixed phase, matter is expected to contain droplets of, negatively charged, kaon-condensed matter immersed in, positively charged, normal matter. However some works suggest that sometimes the GC cannot be satisfied [15] [34]. Here, we study the behavior of the thermodynamic potential in each case of the Maxwell or Gibbs construction, and show that the GC cannot be satisfied in the chiral model as already suggested by Pons et al. [15].

Consider the mixed phase, where the bulk normal matter( $N$ ) and the bulk kaon condensed matter( $K$ ) contact with each other by a sharp boundary<sup>6</sup>. The MC demands the relations

$$\mu_n^N = \mu_n^K, \quad P^N = P^K, \quad (34)$$

on the other hand, the GC can be written as

$$\mu_n^N = \mu_n^K, \quad \mu_e^N = \mu_e^K, \quad P^N = P^K, \quad (35)$$

between two phases. Then we can see that the MC corresponds to the Gibbs construction in the case of only one chemical potential. First of all we figure out how the MC is applied in our study by using thermodynamic potential.

In Fig.9, thermodynamic potential  $\Omega_{total}/V$  is shown as a function of density or  $\langle\theta\rangle$ . The dotted lines in both panels mean the solutions under the equilibrium conditions; chemical equilibrium Eq.(28), local charge neutrality Eq.(30) and equation of motion for kaon

---

<sup>6</sup> We discard any effect given by the boundary or the Coulomb energy.

at momentum zero Eq.(32). Then the dotted lines show the EOS through the relation  $\Omega_{total}/V = -P$  in the left panel, where normal matter with  $\langle\theta\rangle = 0$  exists at low density  $\rho_B < \rho_{crit} = 3.1\rho_0$  and as density increases from  $\rho_{crit}$ , thermodynamically unstable region ( $\partial P/\partial\rho_B < 0$ ) appears up to  $4.5\rho_0$  and the stable region again appears beyond that. On the other hand, the solid lines are calculated with baryon chemical potential fixed ( $\mu_n = 1032, 1082$  and  $1132\text{MeV}$ ), keeping the conditions for chemical equilibrium Eq.(28) and local charge neutrality Eq.(30). In this case the cross points of the solid line with  $\mu_n = 1082\text{MeV}$  and the dotted line in the thermodynamically stable region give the beginning and ending densities of the equal-pressure region in Fig.2. Hence, if we use the MC for the dotted line in the left panel, we get the EOS for the  $T = 0$  and neutrino-free matter in Fig.2. In the right panel, thermodynamic potential in the condensed phase is given as a function of the order parameter  $\langle\theta\rangle$ . The dotted line is given by connecting the extrema satisfying  $\partial\Omega_{total}/\partial\langle\theta\rangle = 0$  in solid lines, which corresponds to the dotted line in the left panel. It is to be noted that the thermodynamically unstable region in the left panel exactly corresponds to the left region to the maximum of the dotted line in the right panel where  $\partial^2\Omega_{total}/\partial\langle\theta\rangle^2 < 0$ . The minimum in each solid line means the ground state; in the case of low  $\mu_n$  the minimum point stays at  $\langle\theta\rangle = 0$ , which means the normal phase is favored. Afterwards two minima appear at  $\mu_n = 1082\text{MeV}$  with equal pressure, corresponding the *coexisting phase*<sup>7</sup> in the context of the MC. Above this value of baryon chemical potential, the kaon condensed phase is always favored.

---

<sup>7</sup> In this section, we call the mixed phase in the case using the MC as the “coexisting phase” and in the case imposing the GC, the “mixed phase” to avoid confusion.

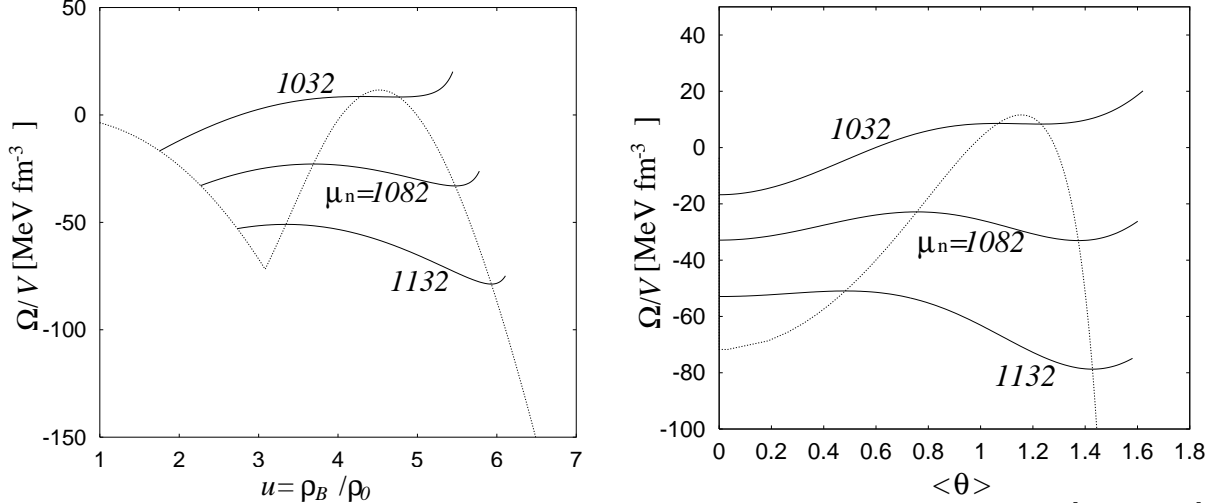


FIG. 9. The behavior of thermodynamic potential is shown as a function of density [left panel] and  $\langle\theta\rangle$  [right panel].  $\mu_n$  is fixed and chemical equilibrium and local charge neutrality are achieved in solid lines. Dotted lines mean the solutions of equilibrium conditions; chemical equilibrium, local charge neutrality and equation of motion for kaon.

Using the MC, typical characteristics are found for the structure of neutron stars as follows; 1: Gravitationally unstable region ( $\partial M_G/\partial\rho_c < 0$ ) appears. 2: There is no *coexisting phase* in neutron stars<sup>8</sup>. 3: Equal-pressure region appears in the EOS and it leads to the density gap in the structure of a neutron star.

These features will disappear when we apply the GC, which is a correct treatment when there exist more than one chemical potential [26]. In order to discuss whether the GC can be satisfied or not, by the similar manner as in the case of the MC, the behavior of thermodynamic potential  $\Omega_{total}/V$  is shown in Fig.10 with two chemical potentials fixed at  $\mu_n = 1082\text{MeV}$  and  $\mu_e = -100, -50, \dots, 150\text{MeV}$ , keeping chemical equilibrium. If the GC can be satisfied, the existence of two minima is expected. However we find only single minimum at  $\langle\theta\rangle = 0$ . Then we can conclude the GC cannot be satisfied in the chiral model [15]. On the other hand, in the meson-exchange model, two minima exist and the GC can be applied except the strong phase transition [15]. The difference between two models results

---

<sup>8</sup> As already we noted in Sect.III B, this comment is correct only when we construct the neutron stars with zero entropy. Finite entropy allows the existence of the *coexisting phase*.

from the nonlinearity of kaon field in the chiral model and we can see that even if we use the weak  $KN$  sigma term, the GC cannot be satisfied in the chiral model<sup>9</sup>.

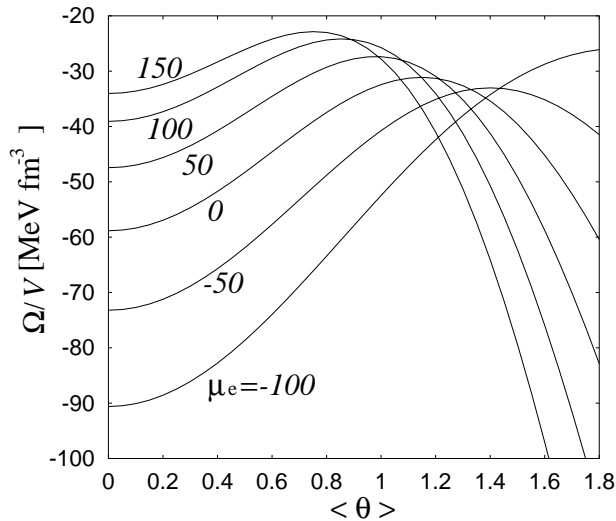


FIG. 10. The behavior of thermodynamic potential is shown as a function of  $\langle\theta\rangle$ . Two chemical potentials are fixed and chemical equilibrium is achieved in each line.

It is to be noted that we have discussed the thermodynamic potential in the ideal situation where the surface and Coulomb effects are discarded. However, this type of argument may miss as essential point for the existence of the mixed phase. When we consider a realistic situation for the mixed phase, there is no clear boundary between two phases; the density of each constituent and the chiral angle should be smoothly changed there. So the naive GC Eq.(35) cannot be applied to this situation. Instead, we must carefully determine the configuration of the mixed phase by allowing the chemical potentials to depend on the spatial coordinates and taking into account the screening effect of the electric potential. Then we can compare the energy of the mixed phase with the normal phase to see whether the mixed

---

<sup>9</sup> Using the chiral model and the “potential energy” contribution Eq.(18) for  $NN$  interaction in non-relativistic approximation, the Gibbs conditions cannot be satisfied, even in the case of the weak  $KN$  sigma term, for example, in the case of  $\Sigma_{KN} = 180\text{MeV}$  where appears very narrow thermodynamically unstable region. It may also be interesting to study the case of relativistic treatment for  $NN$  interaction besides the chiral model for  $KN$  interaction.

phase can exist. Recently there have been appeared some works by taking into account the surface and Coulomb effects along this line [33] [35]. In this treatment, we think, there is some possibility that the chiral model may give the mixed phase as well. This interesting issue is left for a future study.

## REFERENCES

- [1] M. Prakash, I. Bombaci, M. Prakash, P. J. Ellis, J. M. Lattimer and R. Knorren, Phys. Rep. **280** (1997) 1.
- [2] G. E. Brown and H. A. Bethe, Astrophys. J. **423** (1994) 659.
- [3] S.E. Woosley and F.X. Timmers, Nucl. Phys. **A606** (1996) 137.  
L. Zampieri, M. Colpi, S.L. Shapiro and I. Wasserman, Astrophys. J. **505** (1998) 876.  
C.L. Fryer, S.L. Colgate and P.A. Pinto, Astrophys. J. **511** (1999) 885.
- [4] T.W. Baumgarte, S.L. Shapiro and S. Teukolsky, Astrophys. J. **443** (1996) 680.
- [5] W. Keil and H.-Th. Janka, Astron. and Astrophys. **296** (1995) 145.
- [6] J.A. Pons, S. Reddy, M. Prakash, J.M. Lattimer and J.A. Miralles, Astrophys. J. **513** (1999) 780.
- [7] J.A. Pons, J.A. Miralles, M. Prakash and J.M. Lattimer, *astro-ph/0008389*.
- [8] M. Yasuhira and T. Tatsumi, Nucl. Phys. **A663&A664** (2000) 881c.
- [9] D.B. Kaplan and A.E. Nelson, Phys. Lett. **B175** (1986) 57; **B179** (1986) 409(E).
- [10] For review article, C.-H. Lee, Phys. Rep. **275** (1996) 255.
- [11] T. Tatsumi and M. Yasuhira, Phys. Lett. **B441** (1998) 9.
- [12] M. Yasuhira and T. Tatsumi, in *Physics of Hadrons and QCD*, edited by H. Yabu et al., (World Scientific 1999) pp248-251.
- [13] T. Tatsumi and M. Yasuhira, Nucl. Phys. **A653** (1999) 133.
- [14] T. Tatsumi and M. Yasuhira, Nucl. Phys. **A670** (2000) 218c; in *STRANGENESS NUCLEAR PHYSICS* edited by I.-T. Cheon et al., (World Scientific 2000) pp200-207.
- [15] J.A. Pons, S. Reddy, P.J. Ellis, M. Prakash and J.M. Lattimer, Phys. Rev. **C62** (2000) 035803.

- [16] J. Gasser and H. Leutwyler, Phys. Lett. **B188** (1987) 477.  
F.C. Hansen, Nucl. Phys. **B345** (1990) 685.
- [17] V. Thorsson, M. Prakash, J.M. Lattimer Nucl. Phys. **A572** (1994) 693.
- [18] M. Fukugita, Y. Kuramashi, M. Okawa and A. Ukawa, Phys. Rev. **D51** (1995) 5319.  
S.-J. Dong and K.-F. Liu, Nucl. Phys. **B Proc. Suppl.** **42** (1995) 322.
- [19] V. Thorsson and P.J. Ellis, Phys. Rev. **D55** (1997) 5177.
- [20] M. Yasuhira and T. Tatsumi, in preparation.
- [21] M. Prakash, T.L. Ainsworth and J.M. Lattimer, Phys. Rev. Lett. **61**, 2518 (1988).
- [22] T. Takatsuka and J. Hiura, Prog. Theor. Phys. **79** (1988) 268.
- [23] J.I. Kapusta, *Finite-temperature field theory* (Cambridge U. Press, Cambridge, 1989).
- [24] R.I. Epstein and C.J. Pethick, Astrophys. J. **243** (1981) 243.
- [25] N.K. Glendenning, Phys. Rev. **D46** (1992) 1274.
- [26] N.K. Glendenning and J. Schaffner-Bielich, Phys. Rev. Lett. **81** (1998) 4564; Phys. Rev. **C60** (1999) 025803.
- [27] H. Fujii, T. Maruyama, T. Muto and T. Tatsumi, Nucl. Phys. **A597** (1996) 645.
- [28] J.M. Lattimer, C.J. Pethick and D.G. Ravenhall, Nucl. Phys. **A432** (1985) 646.
- [29] T. Takatsuka, Prog. Theor. Phys. **95** (1996) 901.
- [30] T. Muto, T. Tatsumi and N. Iwamoto, Phys. Rev. **D61** (2000) 063001; Phys. Rev. **D61** (2000) 083002.
- [31] T. Muto, T. Tatsumi, N. Iwamoto and M. Yasuhira, in preparation.
- [32] T. Tatsumi, Prog. Theor. Phys. Supplement **91** (1987) 299.
- [33] S. Reddy, G. Bertsch and M. Prakash, Phys. Lett. **B475** (2000) 1.



[34] H. Heiselberg, C.J. Pethick, and E.F. Staubo, Phys. Rev. Lett. **70** (1993) 1355.

[35] T. Norsen and S. Reddy, *nucl-th/0010075*.

M.B. Christiansen, N.K. Glendenning and J. Schaffner-Bielich, *nucl-th/0003045*.